Identification of Chondroitin Polymerizing Factor (CHPF) as Tumor Promotor in Cholangiocarcinoma through Regulating Cell Proliferation, Cell Apoptosis and Cell Migration

Xiaohui Duan
Hunan Provincial People's Hospital, The First-affiliated Hospital of Hunan Normal University
Jianhui Yang
Hunan Provincial People's Hospital, The First-affiliated Hospital of Hunan Normal University
Bo Jiang
Hunan Provincial People's Hospital, The First-affiliated Hospital of Hunan Normal University
Wenbin Duan
Hunan Provincial People's Hospital, The First-affiliated Hospital of Hunan Normal University
Rongguang Wei
Hunan Provincial People's Hospital, The First-affiliated Hospital of Hunan Normal University
Hui Zhang
Hunan Provincial People's Hospital, The First-affiliated Hospital of Hunan Normal University
Xianhai Mao (clinicaldor@sina.com)
Hunan Provincial People's Hospital, The First-affiliated Hospital of Hunan Normal University
https://orcid.org/0000-0003-1377-5246

Primary research

Keywords: cholangiocarcinoma, CHPF, cell proliferation, cell apoptosis, cell migration

Posted Date: June 4th, 2020

DOI: https://doi.org/10.21203/rs.3.rs-32502/v1

Version of Record: A version of this preprint was published at Cell Cycle on March 2nd, 2021. See the published version at https://doi.org/10.1080/15384101.2021.1890951.

Abstract

Background: Cholangiocarcinoma (CCA) is a variety of biliary epithelial tumors involving intrahepatic, perihilar and distal bile duct. It is the most common malignant bile duct tumor in the liver and the second most common primary liver cancer, whose molecular mechanism not fully understood. Specifically, the relationship between CCA and chondroitin polymerizing factor (CHPF) is still not clear.

Methods: In this study, detection of clinical specimens was performed to preliminarily study the role of CHPF in cholangiocarcinoma. Cholangiocarcinoma cells with CHPF knockdown were constructed for *in vitro* study, which was also used in the construction of mice xenograft model for investigating the role of CHPF in the development of cholangiocarcinoma.

Results: The results demonstrated that CHPF was significantly upregulated in cholangiocarcinoma tissues compared with normal tissues. High expression of CHPF was correlated with more advanced tumor grade. Moreover, knockdown of CHPF significantly inhibited cell proliferation, cell migration, promoted cell apoptosis and arrest cell cycle in G2 phase *in vitro*, as well as suppressed tumor growth *in vivo*.

Conclusions: In conclusion, CHPF was identified as a tumor promotor in the development and metastasis of cholangiocarcinoma, which may provide a novel therapeutic target for the targeted therapy against cholangiocarcinoma.

Background

Cholangiocarcinoma (CCA) is a variety of biliary epithelial tumors involving intrahepatic, perihilar and distal bile duct. It is the most common malignant bile duct tumor in the liver and the second most common primary liver cancer, accounting for 10–20% of primary liver cancer [1, 2]. In the past decades, the mobidity and mortality of cholangiocarcinoma are both increasing rapidly worldwide [3]. Moreover, cholangiocarcinoma is usually diagnosed in advanced stage because of its "silent" clinical features [4]. Nowadays, surgery is still the most effective treatment for cholangiocarcinoma, but only 30% of patients are diagnosed with resectable tumor [4, 5]. Even treated with the most aggressive surgery, the recurrence rate of patients with cholangiocarcinoma after resection is still high, which is usually between 67% and 75%, and the 5-year survival rate is still lower than 5% [6]. For patients with advanced or unresectable cholangiocarcinoma, they could only benefit from chemotherapy [7]. However, due to the drawback of drug resistance, the long-term therapeutic effect is still very poor [7, 8]. Therefore, deepening the understanding of molecular mechanism of cholangiocarcinoma is in urgent need for development more effective treatment strategy against cholangiocarcinoma [7, 8].

Chondroitin sulfate (CS), a sulfated glycosaminoglycan, is mainly expressed in connective tissue of human and other animals [9, 10]. Previous studies have demonstrated that CS plays critical role in the regulation of various types of diseases such as osteoarthritis [9, 11], cardiovascular and cerebrovascular diseases [12], central nervous system related diseases [13] and malignant tumors [14]. It was indicated

that CS may execute anti-cancer effects through immunoregulation and inhibiting angiogenesis [15, 16]. The biosynthesis of CS *in vivo* involves several complex steps and 6 glycosyltransferases, among which chondroitin polymerizing factor (CHPF) is an essential cofactor in the synthesis of double disaccharide units in CS mediated by human chondroitin synthase [15, 16]. Except for its role in biosynthesis of CS, CHPF has also been reported to be associated with several types of human cancers [18, 19]. For example, Fan *et al.* showed that, after knocking down the expression of CHPF in glioma cells, cell proliferation was significantly inhibited and cell apoptosis was obviously promoted, which may be attributed to the arrest of cell cycle in G0/G1 phase [20]. However, the role in cholangiocarcinoma played by CHPF has not been reported and remains unclear.

In this study, we identified CHPF as a tumor promotor in the development and progression of cholangiocarcinoma and a potential therapeutic target for cholangiocarcinoma treatment. CHPF was found to be upregulated in cholangiocarcinoma tumor tissues, whose high expression was associated with more advanced malignant grade. The *in vitro* experiments clarified that knockdown of CHPF could inhibit cholangiocarcinoma development through regulating cell growth, apoptosis and migration. The inhibition of cholangiocarcinoma by CHPF knockdown was also confirmed by *in vivo* experiments through constructing mice xenograft models.

Material And Methods

Cell culture, transduction and antibodies

Human cholangiocarcinoma cell lines QBC939, HCCC-9810 and HUCCT1 cells were purchased from BeNa Technology (Hangzhou, Zhejiang, China). QBC939 cells were cultured in 90% DMEM-H medium with 10% FBS containing glutamine and sodium pyruvate. HCCC-9810 and HUCCT1 cells were grow in 90% RPMI-1640 medium with 10% FBS additives containing glutamine. All culture medium was changed every 3 days and cells were humid maintained in a 37 °C 5% CO_2 incubator.

QBC939 and HCCC-9810 cells (2×10^5 cells/mL) were infected with 400μL lentiviral vectors (1×10^7 TU/mL) additive with ENI.S and polybrene (10 μg/mL, Sigma-Aldrich, St Louis, MO, USA) at a MOI of 20 in 6-well plates. After cultured at 37 °C with a 5% CO_2 for 72 h, the fluorescence was observed under microscope with magnification of × 100 and × 200.

Antibodies used in our study were detailed as follows: CHPF (1:100, # ab224495 Abcam) for IHC and CHPF (1:1000), E-cadherin (1:1000, #3195, CST), N-cadherin (1:1000, # ab18203, Abcam), Vimentin (1:1000, # ab92547, Abcam) for WB. Inner control antibody GAPDH (1:3000, # AP0063, Bioworld), and HRP Goat anti rabbit IgG (1:3000, #A0208, Beyotime). Ki-67 (1:200, # Ab16667, Abcam) and HRP Goat anti rabbit IgG (1:400, # ab6721, Abcam) for Ki-67 assay.

Immunohistochemistry (IHC)

Extrahepatic and intrahepatic bile duct adenocarcinoma tissue microarray chip was obtained from Xian Alenabio Co., Ltd (Xian, Shanxi, China), including 74 cases of bile duct adenocarcinoma tissue and 5 cases of bile duct normal tissue. Before the IHC experiment, the tissue microarray chip was baked at 60 °C for 30 min in an oven. Next, the chip was dehydrated in xylene and rehydrated in graded alcohol (100%, 95%, 90%, and 70%). Antigen of the chip was recovered by boiling citric acid buffer for 30 min. After blocked with 3% H_2O_2 and rabbit serum, the chip was incubated with the primary polyclonal antibody of rabbit to CHPF at 4 °C overnight. Subsequently, the chip was washed with PBS three times, and the second antibody was added and incubated for 2 h at room temperature. Finally, the chip was stained with DAB solution for 10 min and counterstained with hematoxylin for 5 min. All tissues in the chip were pictured with microscopic and all slides were viewed with ImageScope and CaseViewer. IHC scores were determined by staining percentage scores and staining intensity scores. Staining percentage scores were classified as: 1 (1%-24%), 2 (25%-49%), 3 (50%-74%), 4 (75%-100%) and staining intensity were scored as 0 (Signalless color), 1 (brown), 2 (light yellow), 3 (dark brown). CHPF expression outcomes in cholangiocarcinoma tissues and para-normal tissues revealed here were analyzed.

Lentiviral vector construction and package

Short hairpin RNA of CHPF was designed in Shanghai Bioscienceres, Co., Ltd (Shanghai, China) and the sequence was 5’-AGCTGGCCATGCTACTCTTTG-3’. The following primer sequences was used for amplifying: Forward, 5’-CCTATTTCCCATGATTCCTTCATA-3’ and reverse, 5’-GTAATACGGTTATCCACGCG-3’. 20 μL PCR volume contained 0.2 μL DNA, 0.4 μL forward primer and 0.4 μL reverse primer and the PCR cycling condition is 94 °C 3 min, 94 °C 30 s, 55 °C 30 s, 72 °C 30 s, 22 cycles, a final extension for 72 °C for 5 min. The PCR products were verified by DNA sequencing and then target sequence was cloned into BR-V-108 lentiviral vector (Shanghai Bioscienceres, China). EndoFree Maxi Plasmid Kit (Tiangen Biotech, Beijing, China) was used for plasmid extraction. Qualified plasmid was used for packaging.

qRT-PCR

Transfected QBC939 and HCCC-9810 cells (LV-shCtrl and LV-shCHPF) were fully lysed and total RNA was extracted using TRIzol reagent (Sigma, St. Louis, MO, USA). Nanodrop 2000/2000C spectrophotometer (Thermo Fisher Scientific, Waltham, MA, USA) was used to evaluate the RNA quality according to the manufacturer’s instructions. Promega M-MLV kit (Heidelberg, Germany) was used to reverse transcribed RNA (2.0 μg) to cDNA. Two steps qRT-PCR was performed with SYBR Green mastermixs Kit (Vazyme, Nangjing, Jiangsu, China) and melting curve was draw, the relative quantitative analysis in gene expression data were analyzed by the $2^{-\Delta\Delta Ct}$ method. GAPDH act as the inner control, and the upstream and downstream primer sequences of human CHPF for the PCR reaction were 5’-GGAACGCACGTACCAGGAG-3’ and 5’-CGGGATGGTGCTGGAATACC-3’, respectively. The upstream and downstream primer sequences of GAPDH were 5’-TGACTTCAACAGCGACACCCA-3’ and 5’-CACCCTGTTGCTGTAGCCAAA-3’.

Western blotting

Lentivirus transfected QBC939 and HCCC-9810 cells (LV-shCtrl and LV-shCHPF) were fully lysed in ice-cold RIPA buffer (Millipore, Temecula, CA, USA) and total protein was collected. The protein concentration was detected by BCA Protein Assay Kit (HyClone-Pierce, Logan, UT, USA). A total of 20 μg per lane was separated by 10% SDS-PAGE (Invitrogen, Carlsbad, CA, USA) and then transferred onto PVDF membranes at 4 °C. The PVDF membranes were blocked with TBST solution containing 5% degreased milk at room temperature for 1 h. Then the PVDF membranes were incubated at 4 °C overnight with primary antibodies. After washing with TBST, the membranes were further incubated with second antibody horseradish peroxidase (HRP)-conjugated Goat anti rabbit IgG for 2 h at room temperature. The blots were visualized by enhanced chemiluminescence (ECL, Amersham, Chicago, IL, USA) and the density of the proteins band was analyzed by ImageJ software.

MTT assay

2500 lentivirus transfected QBC939 and HCCC-9810 cells were seeded into a 96-well plate with 100 mL culture medium. The detection time points were 24 h, 48 h, 72 h, 96 h, 120 h. Four hours before each detection time point, 20 μL 5 mg/mL MTT solution (GenView, El Monte, CA, USA) was added for coloring. After formazan was dissolved by DMSO solution, the absorbance values at 490 nm were measured by microplate reader (Tecan, Männedorf, Zürich, Switzerland) with a reference wavelength of 570 nm. The cell viability ratio was calculated.

Cell apoptosis and cycle assay

Lentivirus transfected QBC939 and HCCC-9810 cells were inoculated in a 6-well plate until cell density reached 85%. Cells were harvested and washed with 4 °C ice-cold PBS. After centrifugation (1200 × g), cells were resuspended with 100 μL binding buffer.

For cell apoptosis, 10 μL Annexin V-APC (eBioscience, San Diego, CA, USA) was added and incubated at room temperature without light. After 15 min later, 300 μL binding buffer was added and apoptosis analyses was measured using FACSCalibur (BD Biosciences, San Jose, CA, USA).

For cell cycle, cells were stained by staining solution containing 40 × PI (2 mg/ml), 100 × RNase (10 mg/ml) and 1 × PBS. FACSCalibur (BD Biosciences, San Jose, CA, USA) was used to detect cell cycle distribution at 200 ~ 300 Cell/s. The percentage of cells in G1, S, and G2-M phases were analyzed.

Wound healing assay

Lentivirus transfected QBC939 and HCCC-9810 cells (5×10^4 cells/well) were plated into a 96-well dish in triplicate for culturing. After confluence of cells reached 90%, the medium was exchanged to medium with

0.5% FBS. Cell scratches across the cell layer were accomplished by a 96 wounding replicator (VP scientific, San Diego, CA, USA). Than the cell layers were gently washed with PBS. 24 h and 48 h post scratching, photographs were taken by a fluorescence microscope and cell migration rates were calculated.

Human Apoptosis Antibody Array

In lentivirus transfected HCCC-9810 cells, the related genes in human apoptosis signal pathway were detected with Human Apoptosis Antibody Array (# ab134001, Abcam, Cambridge, MA, USA) following the manufacturer's instructions. Briefly, lentivirus transfected HCCC-9810 cells at 90% confluence were collected, washed, lysed in ice-cold RIPA buffer (Millipore, Temecula, CA, USA) and then protein concentration was detected by BCA Protein Assay Kit (HyClone-Pierce, Logan, UT, USA). Protein were incubated with blocked array antibody membrane overnight at 4 °C. After washing, 1:100 Detection Antibody Cocktail was added incubating for 1 h, followed by incubated with HRP linked streptavidin conjugate for 1 h. All spots were visualized by enhanced ECL (Amersham, Chicago, IL, USA) and the signal densities were analyzed with ImageJ software (National Institute of Health, Bethesda, MD, USA).

Xenograft mouse model experiments

Female BALB/c nude mice (aged 4 weeks, weighted 17–20 g) obtained from Beijing Vital River Laboratory Animal Technology Co., Ltd. (Beijing, China) were used in our study and the animal experiments were approved by Ethics committee of Hunan Provincial People's Hospital. 4×10^6 LV-shCtrl and LV-shCHPF transfected HUCCT1 cells were subcutaneously injected into the 10 mice which were randomly divided into shCtrl and shCHPF groups. The mice were housed in a conditional environment with a 12-h dark/light cycle. The tumor size and weight of each mouse was monitored 2 times per week. For *in vivo* bioluminescence imaging, all mice were anesthetized by intraperitoneal injection of 0.7% pentobarbital sodium (10 uL/g) 9 weeks post cell injection, and anesthetized mice were placed under the Berthold Technologies living imaging system and imaging was collected. Then anesthetized mice were sacrificed by cervical dislocation and the tumor tissues were harvested for Ki-67 staining assay.

Ki-67 staining assay

Mice tumor tissues were fixed in 10% formalin for 24 h and then were paraffin-embedded. 5 μm slides were cut and immersed in xylene and ethanol for deparaffinization and rehydration. Tissue slides were blocked with 3% PBS-H_2O_2 and were incubated with primary antibody Ki-67 at 4 °C overnight. Then slides were incubated with HRP goat anti-rabbit IgG at room temperature for 2 h. Finally, all slides were stained by Hematoxylin (# BA4041, Baso) for 10 min and Eosin for 5 min (# BA4022, Baso, Zhuhai, Guangdong, China). Stained slides were examined at × 100 and × 200 objective lens microscopic.

Statistical analyses

All cell experiments were performed in triplicate and data were shown as mean ± SD. The significance of the differences between shCHPF and shCtrl group in cells experiment was determined using the two-tailed Student's t-test. Mann-Whitney U analysis and Spearman rank correlation analysis were used while explaining the relationship between CHPF expression and tumor characteristics in patients with cholangiocarcinoma. Statistical significance (*P* value) was calculated by SPSS 22.0 (IBM, SPSS, Chicago, IL, USA) with *P* value < 0.05 as statistically significant. Graphs were made using GraphPad Prism 6.01 (Graphpad Software, La Jolla, CA, USA).

Results

CHPF was highly expressed in cholangiocarcinoma

For exploring the role played by CHPF in the development of cholangiocarcinoma, clinical specimens (including 74 cholangiocarcinoma tissues and 5 normal tissues) were collected and subjected to IHC analysis of CHPF expression. As shown in Fig. 1 and Table 1, CHPF was found to be expressed in both tissues, showing obviously higher expression in cholangiocarcinoma tissues. Simultaneously, it was demonstrated that tumor tissues with higher grade were accompanied with higher expression of CHPF, indicating the potential linkage of them (Fig. 1A). Consistently, the correlation analysis between CHPF expression and tumor characteristics of cholangiocarcinoma patients showed significant association between CHPF expression and malignant grade (Table 2 and Table 3). Altogether, the upregulation of CHPF in cholangiocarcinoma was illustrated, which indicated its potential role in the development of cholangiocarcinoma.

Table 1
Expression patterns of CHPF in cholangiocarcinoma tissues and normal tissues revealed in immunohistochemistry analysis

CHPF expression	Tumor tissue		Normal tissue	
	Cases	Percentage	Cases	Percentage
Low	38	51.4%	5	100%
High	36	48.6%	0	-
P < 0.001				

Table 2
Relationship between CHPF expression and tumor characteristics in patients with cholangiocarcinoma

Features	No. of patients	CHPF expression		*P* value
		low	high	
All patients	74	38	36	
Age (years)				0.492
< 59	36	17	19	
≥ 59	38	21	17	
Gender				0.812
Male	38	19	19	
Female	36	19	17	
Grade				< 0.001***
1	10	10	0	
2	38	26	12	
3	23	0	23	
lymphatic metastasis (N)				0.214
N0	58	32	26	
N1	16	6	10	
T Infiltrate				0.146
T1	5	5	1	
T2	34	17	17	
T3	32	15	17	
T4	3	1	2	

Table 3
Relationship between CHPF expression and tumor characteristics in patients with cholangiocarcinoma analyzed by Spearman rank correlation analysis

Tumor characteristics	index	
Grade	Pearson correlation	0.724
	Significance (two tailed)	< 0.001***
	n	71

Construction of CHPF knockdown cholangiocarcinoma cell lines

Considering the potential facilitation role of CHPF in cholangiocarcinoma, we subsequently silenced CHPF in HCCC-9810 and QBC939 cells to investigate its functions in development of cholangiocarcinoma *in vitro*. ShRNA targeting CHPF (shCHPF), and shCtrl as negative control, were designed, prepared, packaged into lentivirus vector, which was finally used for cell transfection. The fluorescence of green fluorescent protein on lentivirus vector was used as a representation of transfection efficiency, which indicated > 80%, as well as successful transfection (Fig. 2A). Moreover, results of qPCR showed that the mRNA level of CHPF was decreased by 55% and 90% in HCCC-9810 and QBC939 cells, respectively (P< 0.001, Fig. 2B). The successful knockdown of CHPF in HCCC-9810 and QBC939 cells was also verified by the detection of CHPF protein level by western blotting (Fig. 2C). Collectively, these results suggested that the lentivirus expressing shCHPF could significantly downregulate the expression of CHPF in cholangiocarcinoma cells.

Knockdown of CHPF inhibited cell proliferation and induced cell apoptosis and cell cycle arrest

Next, cellular functions were detected in HCCC-9810 and QBC939 cells transfected with shCtrl or shCHPF to reveal the role of CHPF in development of cholangiocarcinoma. It was demonstrated that the viability of cholangiocarcinoma cells was significantly lower in shCHPF group during cell culture, indicating the inhibition of cell proliferation (P< 0.001, Fig. 3A). The detection of cell apoptosis by flow cytometry revealed the significantly increased apoptotic cell percentage in shCHPF group (P< 0.01, Fig. 3B). Moreover, a Human Apoptosis Antibody Array was performed to explore how knockdown of CHPF affects cell apoptosis. The comparison of the expression of apoptosis-related proteins in HCCC-9810 cells with or without CHPF knockdown identify a variety of significantly downregulated proteins, including Bcl-2, CD40, clAP-2, IGF-II, Survivin, sTNF-R1, TNF-β, TRAILR-3, TRAILR-4 and XIAP, and the upregulated Caspase3 (P< 0.05, Fig. 3C). Furthermore, the effects of CHPF on cell cycle distribution were also evaluated for

interpreting its ability to regulate cell apoptosis. Similar results, that CHPF knockdown induced the arrest of cell cycle in S and G2 phase, were obtained in HCCC-9810 and QBC939 cells ($P < 0.05$, Fig. 3D).

Knockdown of CHPF suppressed cell motility and downregulate EMT-related proteins

In order to explore whether CHPF depletion could regulate tumor metastasis of cholangiocarcinoma, cell migration of HCCC-9810 and QBC939 cells transfected with corresponding lentivirus. The outcomes of wound-healing assay showed that knockdown of CHPF could significantly decrease the cell migration ability of HCCC-9810 and QBC939 cells ($P < 0.001$, Fig. 4A). Moreover, as well-known participations in tumor metastasis, epithelial-mesenchymal transition (EMT) related proteins including N-cadherin, Vimentin and Snail were detected in HCCC-9810 and QBC939 cells. As shown in Fig. 4B, the expression levels of N-cadherin and Vimentin showed significant downregulation, while that of E-cadherin exhibited significant upregulation, upon silencing of CHPF, verifying the suppression of EMT as well as tumor metastasis by CHPF knockdown.

CHPF knockdown inhibited tumor growth of cholangiocarcinoma *in vivo*

For the sake of verifying the role of CHPF in cholangiocarcinoma *in vivo*, HUCCT1 cells with or without CHPF knockdown were subcutaneously injected into mice for constructing mice xenograft models. Throughout the culture of animal models, the growth of tumors was observed and the volumes were calculated based on the tumor size. We found that CHPF knockdown could obviously slow down the rate of tumor growth *in vivo* ($P < 0.01$, Fig. 5A). Consistently, the suppression of tumor growth by CHPF knockdown was also visualized by fluorescence imaging which was facilitated by injection of D-Luciferin ($P < 0.05$, Fig. 5B-C). After sacrificing the animals, the weights of tumors were measured, indicating smaller tumors in shCHPF group ($P < 0.01$, Fig. 5D). Besides, Ki-67, which was considered as representation of tumor growth, was also detected in the removed tumors and exhibited apparently downregulation in shCHPF group (Fig. 5E). Altogether, the results suggested that knockdown of CHPF could restrain tumor growth *in vivo*.

Discussion

CS is widely distributed on the extracellular matrix and cell membrane surface of various tissues [10]. It plays an important role in the development of brain neural networks, inflammatory response, infection, cell division and tissue morphology [21]. At the same time, it possesses physiological functions such as inhibiting axonal regeneration after spinal cord injury [22], preventing abnormal myocardial remodeling [23] and so on. Moreover, studies have revealed the capability of CS in the regulation of malignant tumors. For example, it was reported that shark CS could inhibit liver cancer, induce apoptosis of multiple

myeloma and breast cancer cells, and slow down the growth of tumors in mice bearing breast cancer [24]. CHPF is one of the six essential glycosyltransferases in the biosynthesis of CS, which acts as necessary auxiliary factor during the synthesis of repetitive disaccharide unit in CS [10]. Considering the physiological functions of CS, it was supposed that CHPF may regulate cell division and differentiation, thus participating in the regulation of body development and disease occurrence. Moreover, recent studies have revealed the role of CHPF in several types of malignant tumors. Hou *et al.* revealed that knockdown of CHPF could inhibit the development of lung adenocarcinoma *in vitro* and *in vivo* [25]. Besides, they also found the upregulated expression of CHPF in non-small cell lung cancer (NSCLC), and demonstrated the inhibition effects of CHPF silence on cell proliferation, apoptosis and cell cycle, indicating CHPF a potential therapeutic target against NSCLC [26]. Recently, Ye *et al.* identified CHPF as a tumor promotor in esophageal squamous cell carcinoma which was correlated with the prognosis [27]. However, to the best of our knowledge, the functional of CHPF in development of cholangiocarcinoma has not been elucidated.

Through the detection of protein expression of CHPF in cholangiocarcinoma tissues and normal tissues by IHC analysis, we found that CHPF was significantly upregulated in cholangiocarcinoma. Further comparison of CHPF expression between cholangiocarcinoma tissues with different characteristics demonstrated that high CHPF expression was positively correlated with advanced malignant grade, indicating the oncogene-like feature of CHPF in cholangiocarcinoma. Subsequently, *in vitro* experiments demonstrated that knockdown of CHPF significantly slowed down the growth rate, increased the percentage of apoptotic cells, arrest cell cycle in S/G2 phase. Moreover, the promotion of cell apoptosis by CHPF knockdown was contributed to the regulation of various apoptosis-related proteins. Furthermore, we also conducted *in vivo* study through subcutaneously injecting cholangiocarcinoma cells with or without into mice. All the observations in animal study, including the tumor volume, tumor weight, and luciferase imaging demonstrated disturbed tumorigenicity of the cells and the inhibited tumor growth after formation. Altogether, the *in vitro* and *in vivo* studies on the role of CHPF in development of cholangiocarcinoma identified it as a potential tumor promotor.

In addition to malignant proliferation, metastasis is also a major feature of tumor, which seriously restricts the therapeutic effect of tumor and reduces the survival period of patients [28]. Epithelial-mesenchymal transition (EMT) is a process that plays an important role in tumor invasion and metastasis [29–31]. During the process of invasion and metastasis, tumor cells change from epithelial phenotype to mesenchymal phenotype, and thus moving from primary focus to metastasis pathway [32]. E-cadherin and N-cadherin are calcium containing transmembrane glycoprotein, which plays important roles in cell adhesion of epithelial cells. Studies have shown that the progression of EMT is accompanied by simultaneous downregulation of E-cadherin and upregulation of N-cadherin, which can lead to increased invasion and metastasis during tumor progression [33]. For example, the inhibited expression of E-cadherin was identified to mediate the promotion effects of LINC00978 on migration and invasion of hepatocellular carcinoma cells [34]. Consistently, the inhibition of cell migration induced by CHPF deficiency in our study could also be rationalized by the alteration of E-cadherin and N-cadherin. Moreover, Vimentin is an intermediate fibroin expressed by mesenchymal cells, and it is also one of the

important markers of EMT in epithelial cells. Zhu *et al.* presented that CircNHSL1/miR-1306-3p/SIX1 axis could exert its regulatory role in the development and progression of gastric cancer through regulating Vimentin and EMT [35]. Herein, we also found that Vimentin expression was significantly suppressed in cells with CHPF depletion.

Conclusions

Although there are still some limitations in our study, such as limited number of clinical samples and still unclear downstream regulatory mechanism. The results allow us to conclude that CHPF may act as a tumor promotor in the development and progression of cholangiocarcinoma, which may be used as a novel therapeutic target for treating cholangiocarcinoma in the future.

Declarations

Ethics approval and consent to participate

The animal experiments were approved by Ethics committee of Hunan Provincial People's Hospital.

Consent for publication

Not applicable.

Availability of data and material

Not applicable.

Competing interests

The authors declare that they have no competing interests.

Funding

This work was financially supported by Natural Science Foundation of Hunan Province (2019JJ80007 and 2018JJ3294), Key Scientific Research Project of Hunan Provincial Education Department (16A127), and Key Research and Development Project of Hunan Provincial Science and Technology Program (2015sk2050).

Authors' contributions

XM designed this program. XD, JY and BJ operated the cell and animal experiments. XD, WD and RW conducted the data collection and analysis. XD and HZ produced the manuscript which was checked by XM. All the authors have confirmed the submission of this manuscript.

Acknowledgements

This work was financially supported by Natural Science Foundation of Hunan Province, Key Scientific Research Project of Hunan Provincial Education Department, and Key Research and Development Project of Hunan Provincial Science and Technology Program.

References

1. RL Siegel, KD Miller, A Jemal. Cancer statistics, 2019. CA: A Cancer Journal for Clinicians 2019; 69, 7-34.
2. F Bray, J Ferlay, I Soerjomataram, RL Siegel, LA Torre, A Jemal. Global cancer statistics 2018: GLOBOCAN estimates of incidence and mortality worldwide for 36 cancers in 185 countries. CA: A Cancer Journal for Clinicians 2018; 68, 394-424.
3. N Razumilava, GJ Gores. Cholangiocarcinoma. Lancet 2014; 383, 2168-2179.
4. S Rizvi, SA Khan, CL Hallemeier, RK Kelley, GJ Gores. Cholangiocarcinoma - evolving concepts and therapeutic strategies. Nat. Rev. Clin. Oncol. 2017; 15, 95-111.
5. B Doherty, VE Nambudiri, WC Palmer. Update on the Diagnosis and Treatment of Cholangiocarcinoma. Current Gastroenterology Reports 2017; 19, 2.
6. NF Esnaola, JE Meyer, A Karachristos, JL Maranki, ER Camp, CS Denlinger. Evaluation and management of intrahepatic and extrahepatic cholangiocarcinoma. Cancer-Am Cancer Soc 2016; 122, 1349-1369.
7. S Rizvi, GJ Gores. Pathogenesis, Diagnosis, and Management of Cholangiocarcinoma. Gastroenterology 2013; 145, 1215-1229.
8. A Moeini, D Sia, N Bardeesy, V Mazzaferro, JM Llovet. Molecular Pathogenesis and Targeted Therapies for Intrahepatic Cholangiocarcinoma. Clin Cancer Res 2016; 22, 291.
9. N Volpi, F Maccari, V Mantovani. Chondroitin Sulfate and Glucosamine as Disease Modifying Anti-Osteoarthritis Dru gs (DMOADs). Curr Med Chem 2016; 23, 1139-1151.
10. T Mikami, H Kitagawa. Biosynthesis and function of chondroitin sulfate. Biochimica et Biophysica Acta (BBA) - General Subjects 2013; 1830, 4719-4733.
11. M Bishnoi, A Jain, P Hurkat, SK Jain. Chondroitin sulphate: a focus on osteoarthritis. Glycoconjugate J. 2016; 33, 1-13.
12. AV Maksimenko, VL Golubykh, EG Tischenko. Catalase and chondroitin sulfate derivatives against thrombotic effect induced by reactive oxygen species in a rat artery. Metab Eng 2003; 5, 177-182.

13. A Rolls, R Shechter, A London, Y Segev, J Jacob-Hirsch, N Amariglio, et al. Two Faces of Chondroitin Sulfate Proteoglycan in Spinal Cord Repair: A Role in Microglia/Macrophage Activation. Plos Med 2008; 5, e171.
14. S Nadanaka, H Kinouchi, H Kitagawa. Chondroitin sulfates-mediated N-cadherin/β-catenin signaling is associated with basal-like breast cancer cell invasion. J. Biol Chem 2017; 293, 444-465.
15. E Pantazaka, E Papadimitriou. Chondroitin sulfate-cell membrane effectors as regulators of growth factor-mediated vascular and cancer cell migration. Biochimica Et Biophysica Acta 2014; 1840, 2643-2650.
16. AP Asimakopoulou, AD Theocharis, GN Tzanakakis, NK Karamanos. The biological role of chondroitin sulfate in cancer and chondroitin-based anticancer agents. In Vivo 2008; 22, 385-389.
17. H Kitagawa, T Izumikawa, T Uyama, K Sugahara. Molecular Cloning of a Chondroitin Polymerizing Factor That Cooperates with Chondroitin Synthase for Chondroitin Polymerization. J. Biol Chem 2003; 278, 23666-23671.
18. D Kalathas, IE Triantaphyllidou, NS Mastronikolis, PD Goumas, TA Papadas, G Tsiropoulos, et al. The chondroitin/dermatan sulfate synthesizing and modifying enzymes in laryngeal cancer: Expressional and epigenetic studies. Head & Neck Oncology 2010; 2, 27.
19. S Hwang, S Mahadevan, F Qadir, IL Hutchison, DE Costea, E Neppelberg, et al. Identification of FOXM1-induced epigenetic markers for head and neck squamous cell carcinomas. Cancer-Am Cancer Soc 2013; 119, 4249-4258.
20. Y Fan, B Xiao, S Lv, M Ye, X Zhu, M Wu. Lentivirus-mediated knockdown of chondroitin polymerizing factor inhibits glioma cell growth in vitro. Oncol Rep 2017; 38, 1149-1155.
21. T Izumikawa, T Koike, S Shiozawa, K Sugahara, JI Tamura, H Kitagawa. Identification of Chondroitin Sulfate Glucuronyltransferase as Chondroitin Synthase-3 Involved in Chondroitin Polymerization. J. Biol Chem 2008; 283, 11396-11406.
22. A Takeda, S Okada, K Funakoshi. Chondroitin sulfates do not impede axonal regeneration in goldfish spinal cord. Brain Res 2017; 16, 23-29.
23. R Zhao, M Ackers-Johnson, J Stenzig, C Chen, T Ding, Y Zhou, et al. Targeting Chondroitin Sulfate Glycosaminoglycans to Treat Cardiac Fibrosis in Pathological Remodeling. Circulation 2018; 137, 2497-2513.
24. CY Pumphrey, AM Theus, S Li, RS Parrish, RD Sanderson. Neoglycans, carbodiimide-modified glycosaminoglycans: A new class of anticancer agents that inhibit cancer cell proliferation and induce apoptosis. Cancer Res 2002; 62, 3722-3728.
25. X Hou, T Zhang, Z Da, X Wu. CHPF promotes lung adenocarcinoma proliferation and anti-apoptosis via the MAPK pathway. Pathol Res Pract 2019; 215, 988-994.
26. X Hou, Z Baloch, Z Zheng, W Zhang, Y Feng, D Li, et al. Knockdown of CHPF suppresses cell progression of non-small-cell lung cancer. Cancer Manag. Res. 2019; 11, 3275-3283.
27. W Ye, J Zhu, D He, D Yu, H Yang, W Wang, et al. Increased CDKL3 expression predicts poor prognosis and enhances malignant phenotypes in esophageal squamous cell carcinoma. J. Cell Biochem 2019;

120, 7174-7184.
28. KT Yeung, J Yang. Epithelial-mesenchymal transition in tumor metastasis. Mol. Oncol. 2017; 11, 28-39.
29. M Diepenbruck, G Christofori. Epithelial-mesenchymal transition (EMT) and metastasis: yes, no, maybe? Curr Opin Cell Biol 2016; 43, 7-13.
30. TT Liao, MH Yang. Revisiting epithelial-mesenchymal transition in cancer metastasis: the connection between epithelial plasticity and stemness. Mol. Oncol. 2017; 11, 792-804.
31. F Marcucci, G Stassi, RD Maria. Epithelial|[ndash]|mesenchymal transition: a new target in anticancer drug discovery. Nat Rev Drug Discov 2016; 15, 311-325.
32. L Samy, X Jian, D Rik. Molecular mechanisms of epithelial-mesenchymal transition. Nat Rev Mol Cell Bio 2014; 15, 178-196.
33. Loh, Chai, Tang, Wong, Sethi, Shanmugam, et al. The E-Cadherin and N-Cadherin Switch in Epithelial-to-Mesenchymal Transition: Signaling, Therapeutic Implications, and Challenges, Cells-Basel 2019; 8, 1118.
34. X Xu, J Gu, X Ding, G Ge, X Zang, R Ji, et al. LINC00978 promotes the progression of hepatocellular carcinoma by regulating EZH2-mediated silencing of p21 and E-cadherin expression, Cell Death Dis. 2019; 10, 752.
35. Z Zhu, Z Rong, Z Luo, Z Yu, J Zhang, Z Qiu, et al. Circular RNA circNHSL1 promotes gastric cancer progression through the miR-1306-3p/SIX1/vimentin axis, Mol. Cancer 2019; 18, 126.

Figures

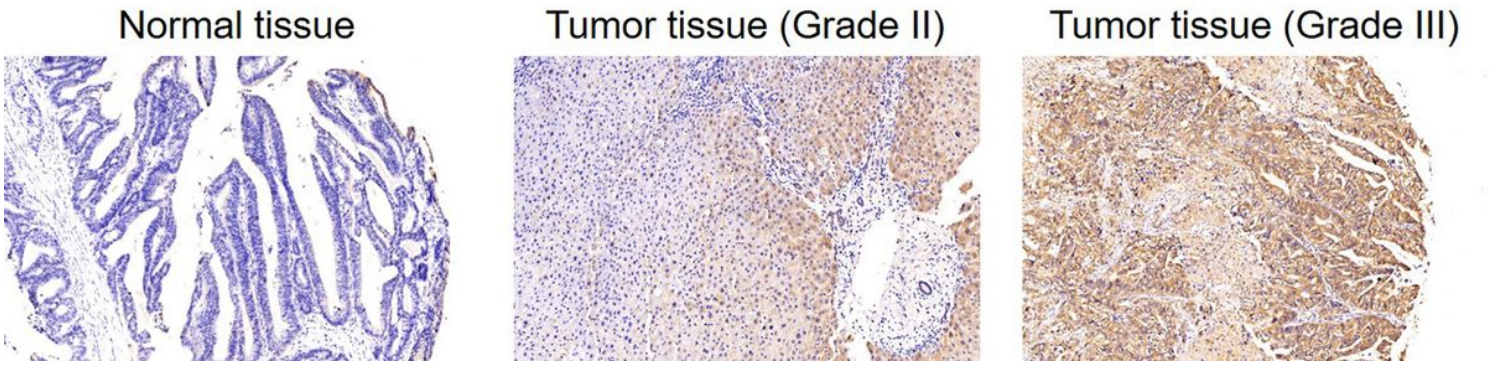

Figure 1

CHPF was upregulated in cholangiocarcinoma. The expression of CHPF in tumor tissues of cholangiocarcinoma was detected by IHC and compared with normal tissues, showing that CHPF was upregulated in cholangiocarcinoma and associated with tumor grade. The representative images were randomly selected from at least 3 independent experiments.

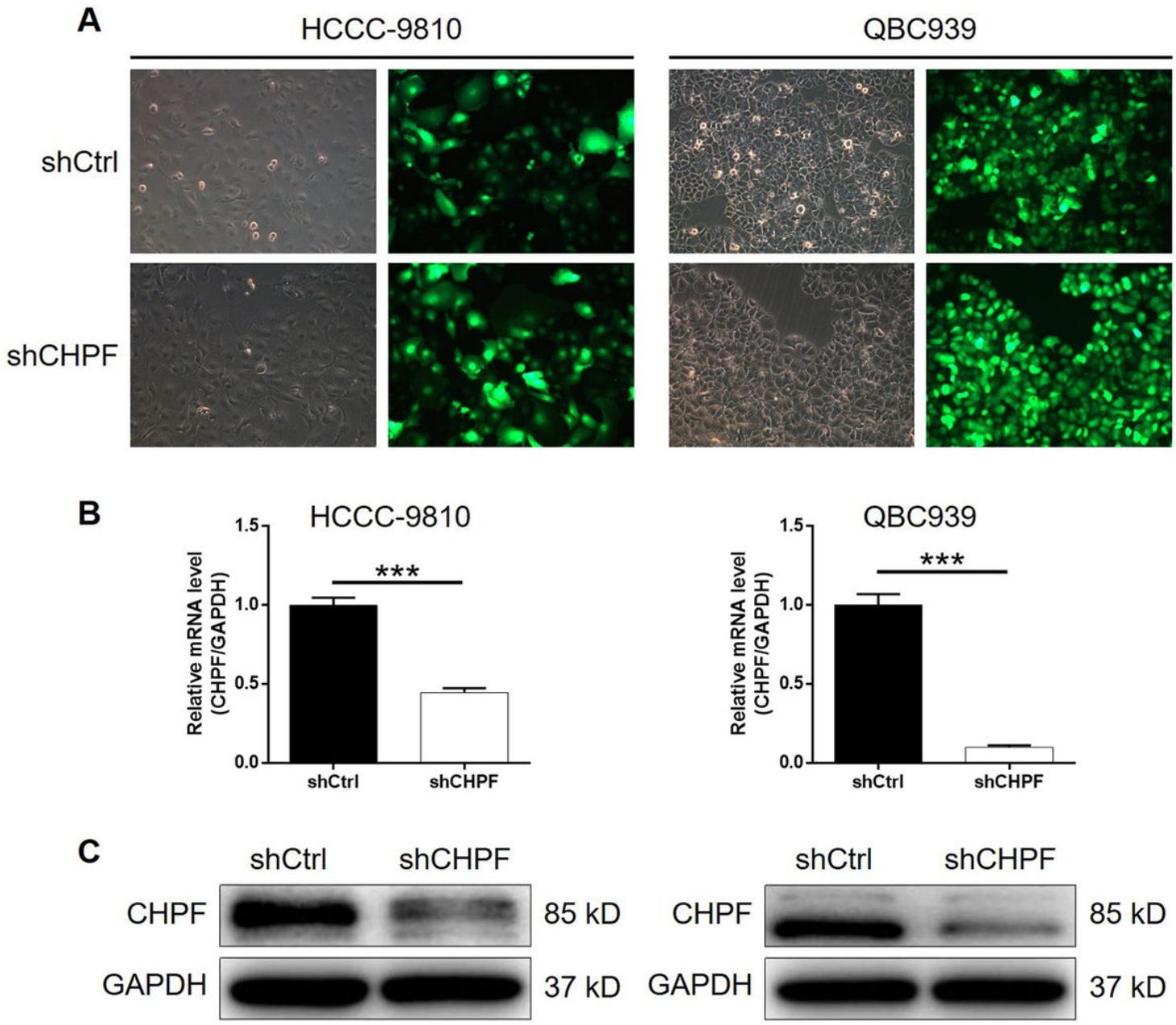

Figure 2

Construction of cholangiocarcinoma cell models with CHPF knockdown. (A) Fluorescence imaging was performed to evaluate the efficiency of lentivirus transfection. (B) qPCR was utilized to detect the knockdown efficiency of CHPF in HCCC-9810 and QBC939 cells. (C) The successful knockdown of CHPF in HCCC-9810 and QBC939 cells was further verified by western blotting. The representative images were randomly selected from at least 3 independent experiments. The data was shown as mean ± SD. *P < 0.05, **P < 0.01, ***P < 0.001

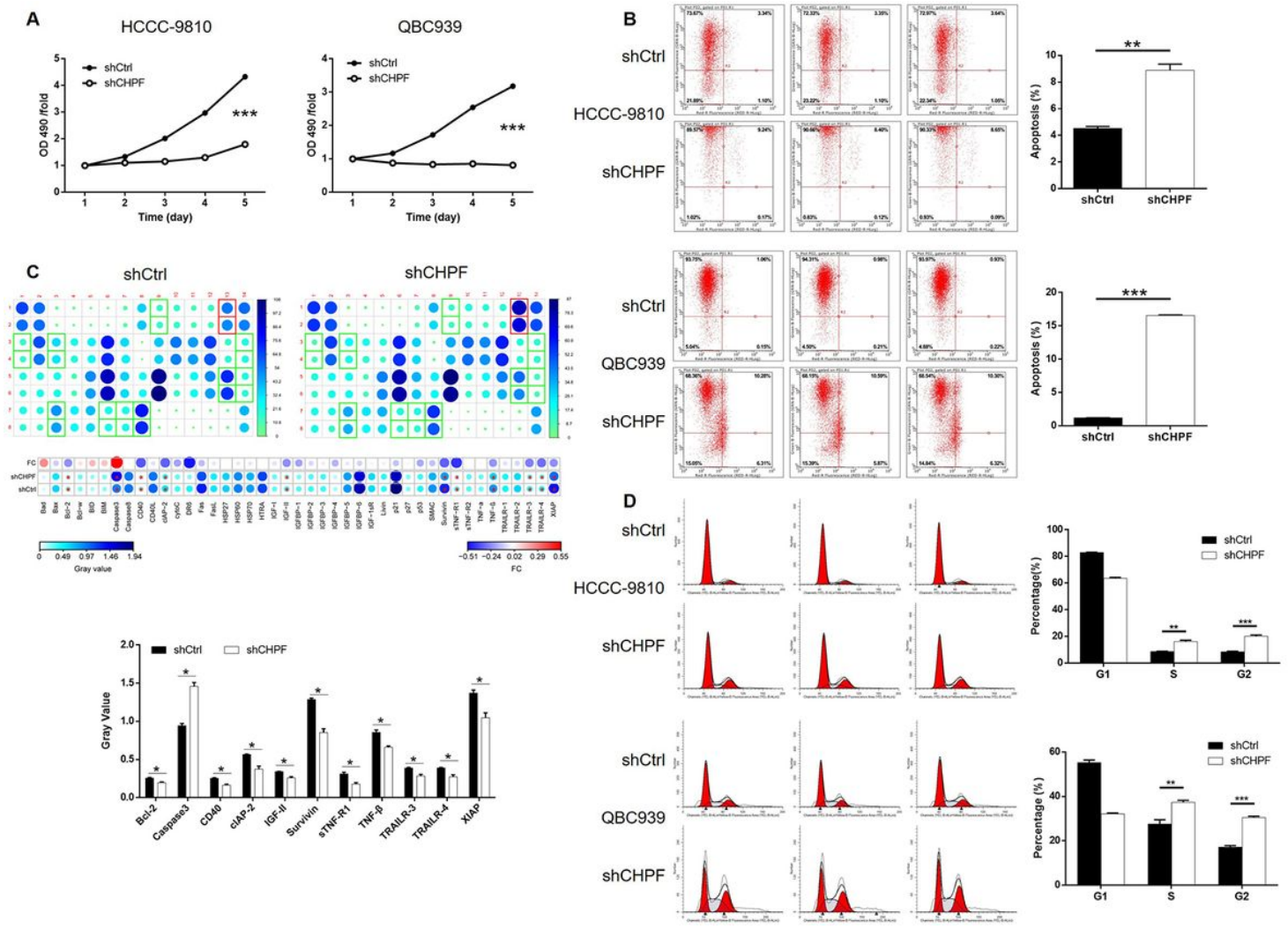

Figure 3

CHPF knockdown inhibited cell proliferation and promoted cell apoptosis and cell cycle arrest in cholangiocarcinoma cells. (A) MTT assay showed that knockdown of CHPF significantly inhibited cell proliferation of HCCC-9810 and QBC939 cells. (B) The results of flow cytometry demonstrated that knockdown of CHPF obviously promoted cell apoptosis of HCCC-9810 and QBC939 cells. (C) Human Apoptosis Antibody Array was performed to identify the differential expression of apoptosis related proteins between shCtrl and shCHPF groups of HCCC-9810 cells. (D) The detection of cell cycle indicated that knockdown of CHPF significantly promoted the arrest of cell cycle in G2 phase. The data was shown as mean ± SD. *P < 0.05, **P < 0.01, ***P < 0.001

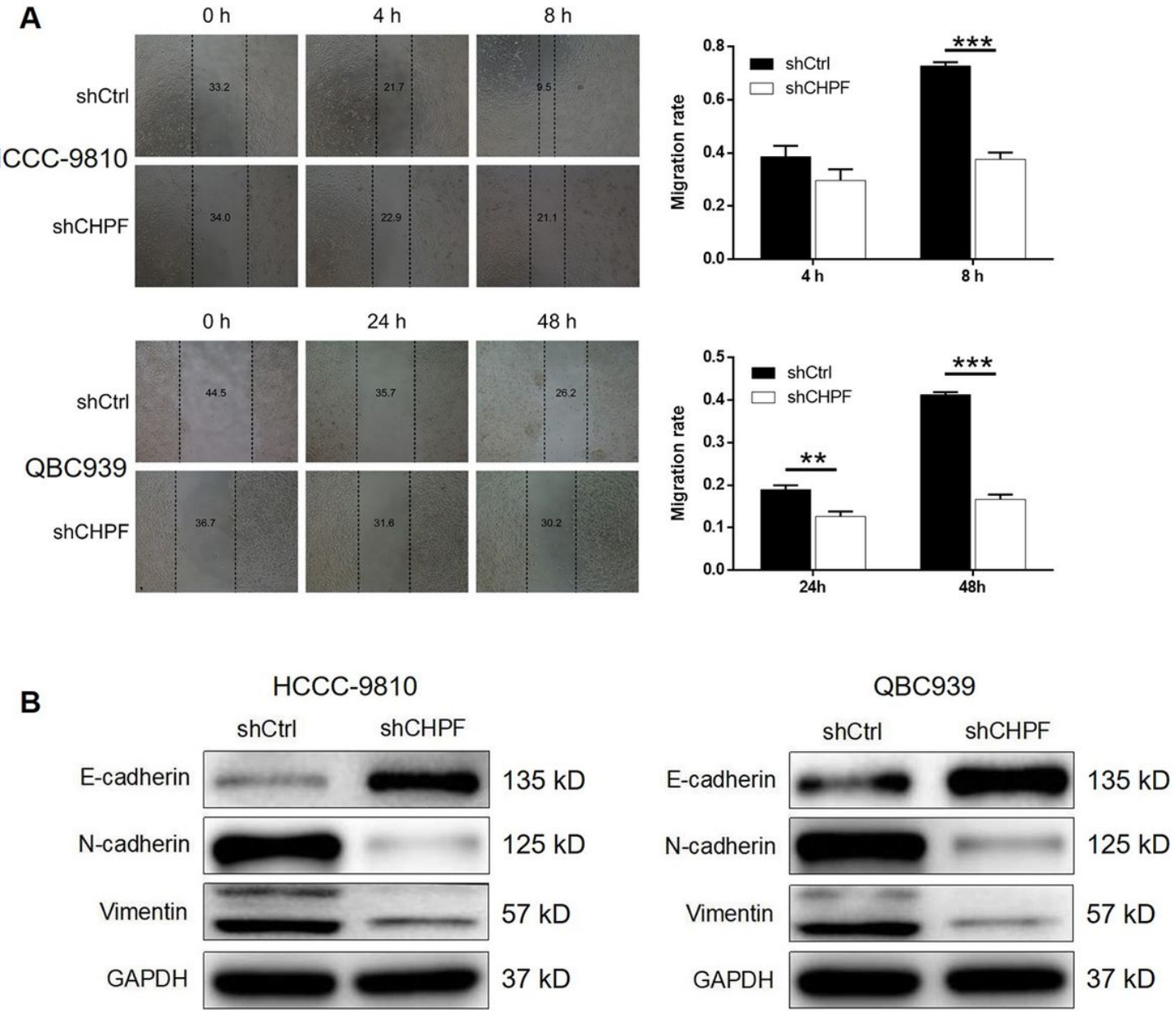

Figure 4

CHPF knockdown inhibited cell migration and expression of EMT-related proteins. (A) Wound-healing assay showed that cell migration of HCCC-9810 and QBC939 cells was significantly suppressed by CHPF knockdown. (B) The results of western blotting showed the downregulation of EMT-related proteins in shCHPF group of both HCCC-9810 and QBC939. The representative images were randomly selected from at least 3 independent experiments. The data was shown as mean ± SD. *P < 0.05, **P < 0.01, ***P < 0.001

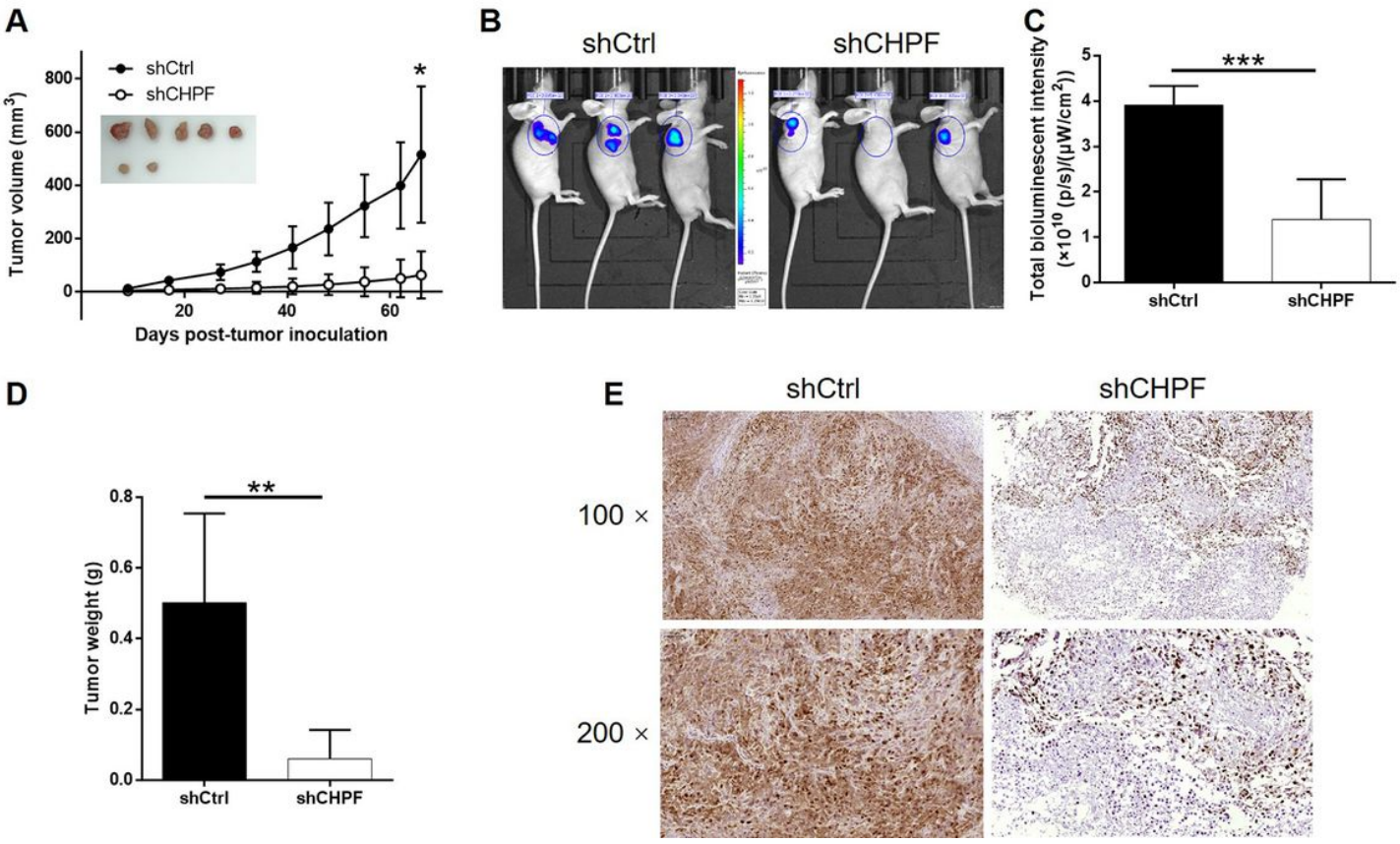

Figure 5

CHPF knockdown inhibited tumor growth of cholangiocarcinoma in vivo. (A) Volume of tumors was measured and calculated throughout the culture of animal models and showed obviously showed down growth of tumor in shCHPF group. Inset showed the photo of the removed tumors. (B, C) The bioluminescence intensity obtained by in vivo imaging showed apparently smaller tumors in shCHPF group. (D) The weight of the tumors was measured, which showed that tumors in shCHPF group were lighter. (E) The IHC analysis of Ki-67 expression in tumors showed obvious higher levels in shCtrl group. The representative images were randomly selected from at least 3 independent experiments. The data was shown as mean ± SD. *P < 0.05, **P < 0.01, ***P < 0.001